



# Energy harvesting from low-frequency sinusoidal vibrations using diaphragm type piezoelectric element

Nitin Yadav & Rajesh Kumar\*

Department of Mechanical Engineering, Sant Longowal Institute of Engineering and Technology, Longowal 148 106, India

Received: 13 July 2020; Accepted: 26 March 2021

Piezoelectric has great potential in energy harvesting. In the present work, investigations have been made on harvesting mechanical vibration energy by a diaphragm type piezoelectric element. The piezoelectric element has been placed at the center of a fix-free-fix-free rectangular plate. Excitation to the plate in the range of 10 Hz-150 Hz frequencies and 10 mVpp to 150 mVpp amplitude has been applied by a model exciter. The output from piezoelectric element has been measured in terms of current and voltage. The experimental results have revealed that the power output of piezoelectric increases with an increase in input amplitude. However, at constant input amplitude (150 mVpp) in the frequency range 10 Hz to 150 Hz, the power output has attained its maximum value (902  $\mu$ W) at frequency 60 Hz. Further, the energy harvesting capabilities have also been investigated near the natural frequency band of the structure. The results have showed that in the natural frequency band, even a low amplitude excitation can also increase power output from the piezoelectric element. It has been concluded that using a piezoelectric element, vibration energy can be converted into electrical energy to operate small gadgets.

**Keywords:** Diaphragm, Energy harvesting, Piezoelectric, Plate structure, Vibration

## 1 Introduction

Advancement in technology has prompted rapid development in small gadgets, devices and sensors. Usually, small batteries fulfil the power requirements of such devices. The batteries have limited life span. So, there is a need for a system that can power these small sensors or gadgets continuously by capturing some energy from the system or environment itself. Solar cells are an option as an energy producer for the devices which are used in open and remote areas. But solar cells have also a drawback of their dependability on sunlight. Nowadays, researchers are utilizing vibrations for energy harvesting. Literature is available in which principle of piezoelectric, electrostatic and electromagnetic<sup>1-7</sup> have been utilized to produce electric power from vibrations and vice versa. A comparative study of these three principles shows that the piezoelectric principle is quite simple, easy, and well capable of generating power for low energy devices<sup>1,8,9</sup>. In some cases, magnate based systems have been hybridized with the piezoelectric principle to harvest the energy<sup>10</sup>. Piezoelectric is the materials that produce electric potential due to variation in their physical structure, which may be due to vibration or some movement in the system. Several studies have

been made on human shoe<sup>11-12</sup>, heart<sup>13</sup>, and powering of the pacemaker by using heartbeat movement<sup>14</sup>, knee<sup>15</sup>, arms and skin<sup>16</sup> etc. for power production from human motion and in the area of hydropower<sup>17</sup> as well for the same purpose. Attempts have also been made to utilize vehicle vibrations like that of aeroplane wings, shaft, tire, the suspension system of vehicles, and engine for energy harvesting<sup>18-23</sup>. The above-discussed energy harvesting systems have piezoelectric elements layered on one side<sup>6</sup> or both sides of beam<sup>24</sup>, cymbal disc<sup>25</sup>, ring structure<sup>26</sup>, and diaphragm<sup>27-31</sup>. Schematic of a typical diaphragm type piezoelectric element is shown in Fig. 1.

In the present work, the utility of a diaphragm type piezoelectric element in energy harvesting under low vibration conditions has been studied. The piezoelectric element has been placed at the center of a fix-free-fix-free rectangular plate. The effect of plate excitation on the power output of the piezoelectric element has been investigated. The effect has also been investigated in the natural frequency band of the vibrating plate.

## 2 Materials and Methods

### 2.1 Mathematical formulation

The output from the piezoelectric energy harvesting system depends on the mechanical and electrical

\*Corresponding author (E-mail: rajesh\_krs@sliet.ac.in)

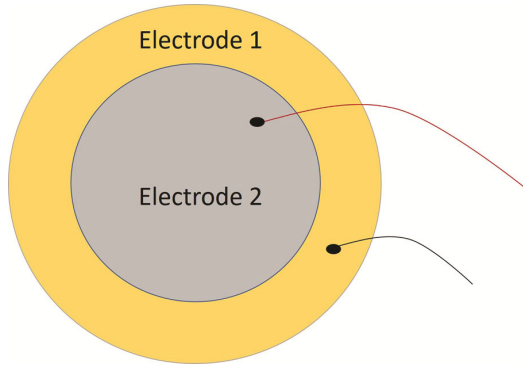


Fig. 1 — A typical diagram of the piezoelectric diaphragm.

properties of different components of the piezoelectric system. The system works based on either direct principle or reverse principle. The basis of the direct principle is that the force is applied to the piezoelectric element, and output is obtained in terms of electricity. On the other hand, in reverse principle, electrical input is given to the piezoelectric element to produce some mechanical deformation.

The strain (S) in the mechanical system, as per reverse principle, can be described in terms of the electric field in the piezoelectric system<sup>32</sup> as given in Eq. (1).

$$S_{ab} = s_{abcj}^E \sigma_{cj} + d_{cab} E_c \quad \dots(1)$$

where, S is strain in the mechanical system (dimensionless), E is electric field in the piezoelectric system (V/m or N/C),  $\sigma$  is stress in the mechanical system (N/m<sup>2</sup>), s is mechanical compliance (m<sup>2</sup>/N), and d is strain tensor of the piezoelectric element in (C/N) which is also termed as the piezoelectric coefficient.

According to the direct principle of the piezoelectric system, the electric displacement, D in C/m<sup>2</sup> is expressed as given in Eq. (2).

$$D_{ab} = d_{abcj} \sigma_{cj} + \varepsilon_{ac}^T E_c \quad \dots(2)$$

where,  $\varepsilon$  is dielectric permittivity (F/m), and a, b, and c are indices for x, y and z directions respectively whereas j indicates shear to y-z direction.

The direct principle of the piezoelectric system is used in the present research for energy harvesting. The tensor Eq. (2) for this can be represented in the matrix form as in Eq. (3).

$$\{D\} = [d](\sigma) + [\varepsilon^T]\{E\} \quad \dots(3)$$

At the time of the initiation electric field, E is zero. Hence, the Eq. (3) can be simplified and given in Eq. (4) as

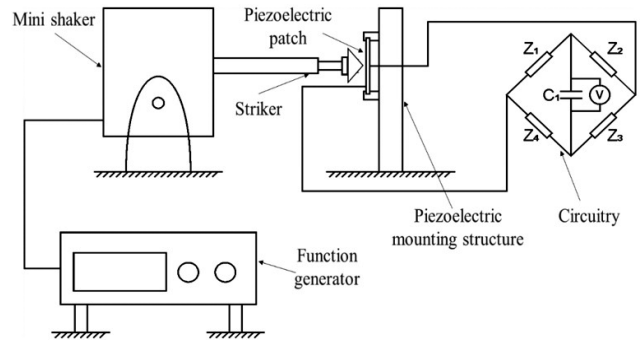


Fig. 2 — A schematic diagram of the experimental setup.

$$\{D\} = [d](\sigma) \quad \dots(4)$$

Hence, total electric charge (C) per unit area is written in the form of piezoelectric coefficient (C/N), and Force (N) as in Eq. 5.

$$C = \text{Piezoelectric coefficient} * \text{Force} \quad \dots(5)$$

As the capacitance of piezoelectric material is C/V, Eq. (5) can be rewritten in the form of Eq. (6).

$$\text{Voltage output (V)} = \frac{\text{Piezoelectric coefficient} \left(\frac{C}{N}\right) * \text{Force(N)}}{\text{Capacitance} \left(\frac{C}{V}\right)} \quad \dots(6)$$

In the case of vibration, the force (N) is dynamic. Current and power produced by piezoelectric elements can be calculated considering Eq. (6) and the value of resistance of the piezoelectric circuit.

### 2.2 Experimental procedure

The study of the effect of low sinusoidal vibrations on a diaphragm type piezoelectric element was performed on a specifically designed experimental setup. It consists of a function generator, smart mini shaker, diaphragm type piezoelectric element, constrained plate support, electric circuit, and a multimeter. The schematic of the experimental setup is shown in Fig. 2. A typical photograph of the setup and plate holding element are shown in Fig. 3(a and b). The smart mini shaker (Model no. K2004E01, Make: TMS) was used to vibrate the piezoelectric element mounted on a fix-free-fix-free plate made of mild steel. A concentrated (point) dynamic load was applied to the piezoelectric element placed at the centre of the plate. The amplitude and frequency of the applied load were as per the input signal given to the shaker through a function generator (Model no. 33220A, Make: Agilent). The two opposite ends of

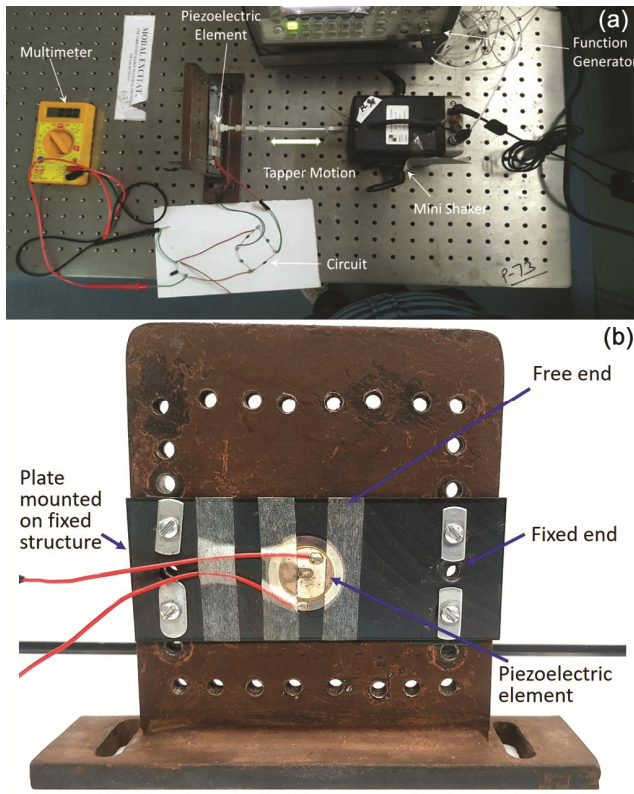


Fig. 3 — Photograph of (a) excitation of piezoelectric by a shaker, and (b) fixed-free-fixed-free condition of plate used in the experimental setup.

the plate were fixed by nuts-bolts, and the remaining ends were free. Type of structure and boundary conditions can be decided considering desired working range<sup>33</sup>. The effective dimension of the plate structure was 82 mm × 50 mm × 0.6 mm. The diaphragm type piezoelectric element was made of PZT (Lead Zirconate Titanate) material with nickel alloy electrode of dimension 28 mm outer diameter and 0.15 mm thickness. A full-wave bridge rectifier circuit was used for converting alternating current into direct current. In this bridge rectifier, four diodes of 4.5 ohms and a capacitor of 16  $\mu\text{F}$  were used for charge storage. A multimeter was used for measuring the voltage and current output from the piezoelectric energy harvester.

### 3 Results and Discussion

Studies were conducted to know the effect of amplitude and frequency of excitation on the output from the piezoelectric element.

In the first study, a force at a constant frequency (much away from natural frequency) and varying amplitude were applied to the piezoelectric element. Mechanical systems normally go under low-frequency

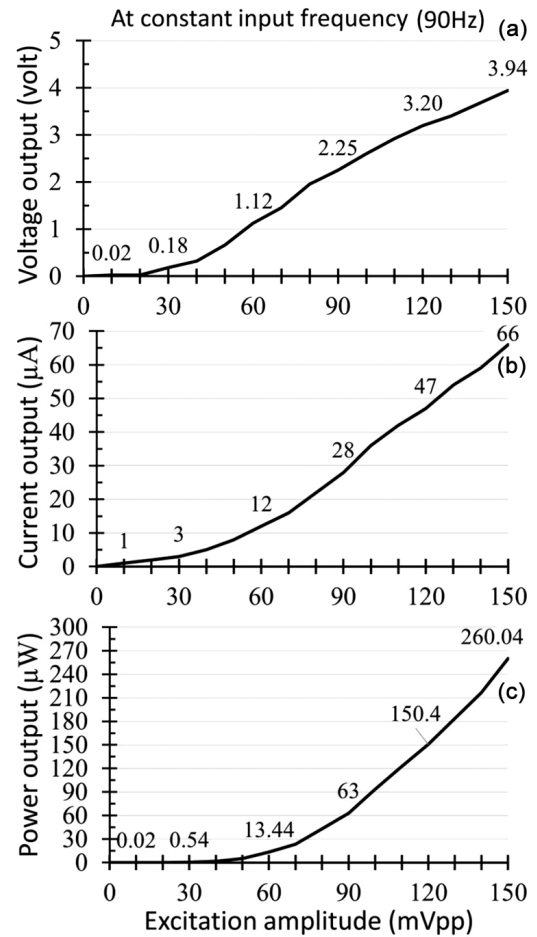


Fig. 4 — Plot at constant input frequency (90 Hz) for excitation amplitude (mVpp) versus piezoelectric output in terms of (a) voltage (volt), (b) current ( $\mu\text{A}$ ), and (c) power ( $\mu\text{W}$ ).

conditions. To simulate such conditions, experiments were conducted at frequency 90 Hz, and the amplitude was varied in the range of 10 mVpp to 150 mVpp. The plot between the excitation amplitude and the output voltage of the piezoelectric element is shown in Fig. 4(a). The trend is similar to the plot for the variation in force and output voltage of PZT on the touch-pad<sup>34</sup>. From the plot, it has been observed that with an increase in the force of excitation, the output voltage is increased. It is due to the reason that the larger force results in larger deformation in the piezoelectric material structure, which leads to the generation of increased electric potential. Graph showing variation in output current and power for the excitation amplitude is given in Fig. 4(b and c), respectively. In both the cases, an increase in output has been noticed with an increase in excitation amplitude. At excitation amplitude 150 mVpp, the output current was recorded as 66  $\mu\text{A}$  and power as 260  $\mu\text{W}$ .

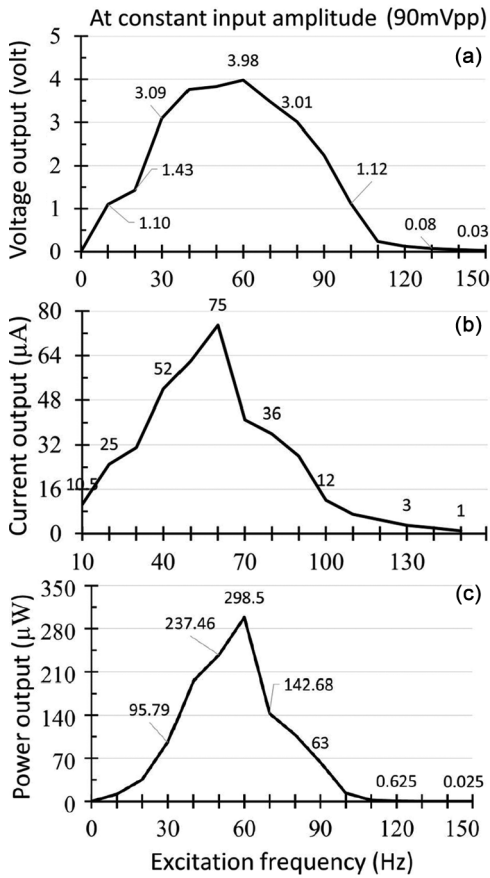


Fig. 5 — Plot at constant input amplitude (90 mVpp) for outputs (a) voltage (volt) versus excitation frequency (Hz), (b) current ( $\mu\text{A}$ ) versus excitation frequency(Hz), and (c) power ( $\mu\text{W}$ ) versus excitation frequency (Hz).

In the second study, a force at constant amplitude and varying frequency were applied on the diaphragm to characterize its frequency response. In this study, the excitation force was kept constant at 90 mVpp, and frequency was varied from 10 Hz to 150 Hz. The effect of change in excitation frequency on the output voltage of the diaphragm is shown in Fig. 5(a). The figure indicates that maximum output voltage 3.98 volt was obtained at 60 Hz. The trend is comparable with the results available in the literature<sup>35-37</sup>. Plots for output current and power for the excitation frequency are also shown in Fig. 5(b) and Fig. 5(c), respectively. The maximum values of output current and power was obtained as 75  $\mu\text{A}$  and 298  $\mu\text{W}$ , respectively, at 60 Hz. Further, studies were extended to map different amplitude and frequencies in the range of 10 mVpp - 150 mVpp and 10 Hz – 150 Hz, respectively. The result of output voltage, current, and power corresponding to each input excitation is shown in the form of surface graphs in Fig. 6(a-c).

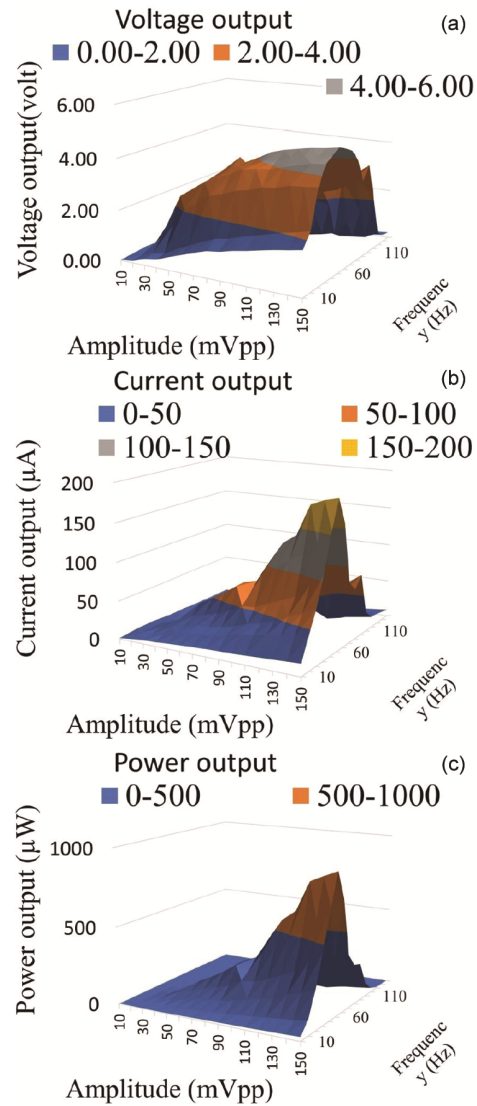


Fig. 6 — Surface graph of (a) voltage output(volt), (b) current output ( $\mu\text{A}$ ), and (c) power output ( $\mu\text{W}$ ) corresponding to different input amplitudes (mVpp) and frequencies (Hz).

The maximum output power was obtained for the combination of excitation amplitude and frequency as 150 mVpp and 60 Hz, respectively.

In the third study, the response in the band of natural frequency was analyzed. An estimate of a natural frequency for a given constrained plate was evaluated using finite element method and verified experimentally with the help of accelerometer, data acquisition system, and Lab VIEW software. The simulation result of finite element analysis at first natural frequency is shown in Fig. 7. The first natural frequency as per the simulation results was estimated at 492 Hz, and maximum displacement was at the center of the plate.

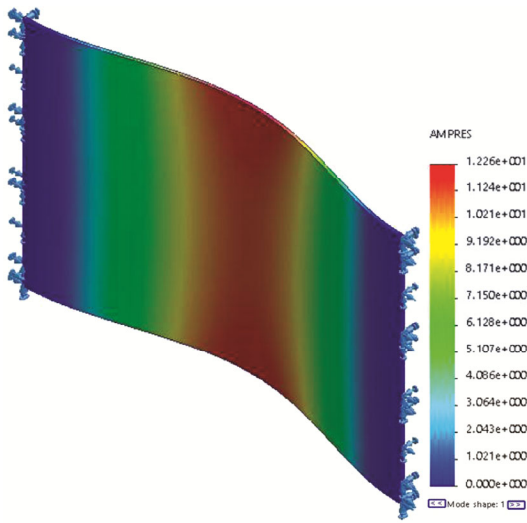


Fig. 7 — Deformation in the plate at first mode of natural frequency.

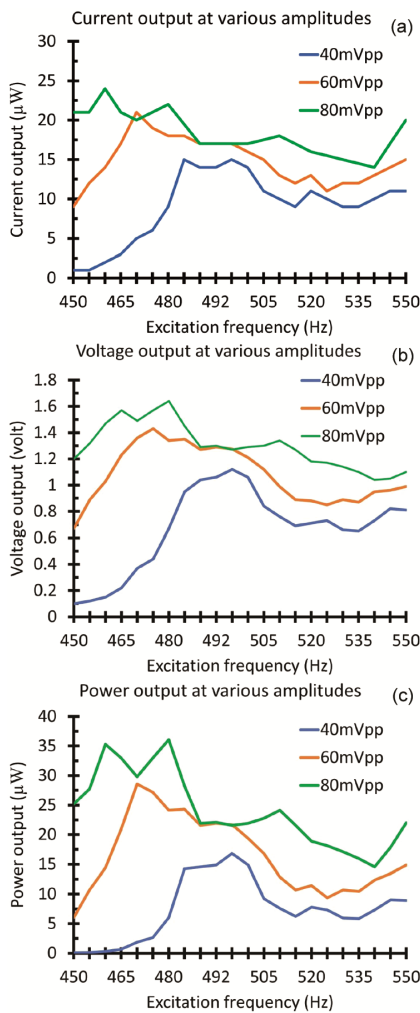


Fig. 8 — (a) Current output ( $\mu\text{A}$ ) versus frequency(Hz), (b) voltage output (volt) versus frequency(Hz), and (c) power output( $\mu\text{W}$ ) versus frequency (Hz) at different amplitudes(mVpp).

From experiments, the first natural frequency was observed at 487 Hz. The variation in experimental and simulation results might have occurred due to the realistic clamping conditions and non-uniform material properties across the plate. Such variations were also reported during vibration studies of the plate by digital speckle pattern interferometry<sup>38,39</sup>.

Further, the data were collected in the input frequency band of 450 Hz to 550 Hz, so that effect of the natural frequency band could also be recorded. In this study, the amplitude was varied from 10 mVpp to 90 mVpp. The output from the piezoelectric element in the form of current, voltage, and power are shown in Fig. 8(a-c). From graphs, it is concluded that the power output near natural frequency (492 Hz) is very close for different input amplitude. This indicates that even the low amplitude vibration at a natural frequency can generate sufficient power output from the piezoelectric element. However, in the natural frequency band but away from the natural frequency, increased input vibration amplitude resulted in increased power output.

As the power output depends on both the amplitude and frequency of vibration, within the given constrains, by the adjustment of amplitude and frequency one can optimize power output.

#### 4 Conclusion

The possibility of harvesting electrical energy from low-frequency mechanical vibrations through the piezoelectric element has been explored. Investigations have been made on the specified plate with fix-free-fixed-free boundary conditions excited in the range of frequency 10 Hz - 150 Hz and amplitude 10 mVpp - 150 mVpp. The maximum output has been obtained at 60 Hz frequency and 150 mVpp amplitude. The voltage output from piezoelectric, in this case, has been 4.75 volt. It has been observed that when vibration is in the natural frequency band, even low amplitude input results in significant power output from a piezoelectric element.

The investigated energy harvesting system can be used effectively as a power support for small electrical and electronic gadgets such as mobile charging and glowing LEDs. Investigations on change in dimensions of the plate and the boundary constraints can be made to increase deflections and power output as a future scope of the work.

#### Acknowledgment

Nitin Yadav is thankful to Sant Longowal Institute of Engineering and Technology for providing fellowship under TEQIP III.

## References

- 1 Boisseau S, Despesse G, & Ahmed B, in *Small-Scale Energy Harvesting*, edited by Lallart M (Intech open, Croatia), ISBN 978-953-51-0826-9, (2012) 91.
- 2 Torres E O, & Rincón-Mora G A, *IEEE J Solid-State Circuits*, 45 (2010) 483.
- 3 Kulkarni S, Roy S, O'Donnell T, Beeby S, & Tudor J, *J Appl Phys*, 99 (2006) 7.
- 4 Harne R L, & Wang K W, *Smart Mater Struct*, 22 (2013) 023001.
- 5 Kim H S, Kim J H, & Kim J, *Int J Precis Eng Manuf*, 12 (2011) 1129.
- 6 Guo H, Li J, Wang Y, Wang Y, & Li Y, *J Vib Eng Technol*, 7 (2019) 389.
- 7 Vashist S K, & Chhabra D, *Proc SPIE*, 9057 (2014) 905720-1.
- 8 Siddique A R M, Mahmud S, & Heyst B V, *Energy Convers Manag*, 106 (2015) 728.
- 9 Renaud M, Karakaya K, Sterken T, Fiorini P, Hoof C V, & Puers R, *Sens Actuators A*, 145-146 (2008) 380.
- 10 Noll M U, Lentz L, & Wagner U V, *J Vib Eng Technol*, 8 (2020) 285.
- 11 Shenck N S, & Paradiso J A, *IEEE Micro*, 21 (2001) 30.
- 12 Rocha J G, Gonçalves L M, Rocha P F, Silva M P & Lanceros-Méndez S, *IEEE Trans Ind Electron*, 57 (2010) 813.
- 13 Deterre M, Boutaud B, Dalmolin R, Boisseau S, Chaillout J-J, Lefeuvre E, & Dufour-Gergam E, *Proc Symp DTIP*, (2011) 387.
- 14 Barman A, Dutta T, & Dey D, *J Phys: Conf Ser*, 1797 (2021) 012037.
- 15 Pozzi M, & Zhu M, *Smart Mater Struct*, 21 (2012) 055004.
- 16 Yuan H, Lei T, Qin Y, & Yang R, *Nano Energy*, 59 (2019) 84.
- 17 Yadav N, & Chhabra D, *J Control Instrum*, 8 (2018) 30.
- 18 Buchacz A, & Gałęziowski D, *Indian J Eng Mater Sci*, 23 (2016) 425.
- 19 Anton S R, & Inman D J, *Proc SPIE*, 6928 (2008) 692824-1.
- 20 Pillatsch P, Yeatman E M, & Holmes A S, *Sens Actuators A*, 206 (2014) 178.
- 21 Lee J, & Choi B, *Energy Convers Manag*, 78 (2014) 32.
- 22 Khalatkar A, Gupta V K, & Agrawal A, *Smart Mater Res*, 2014 (2014) 1.
- 23 Tavares R, & Ruderman M, *Mechatronics*, 65 (2020) 102294-1.
- 24 Deng J, Guasch O, Zheng L, Song T, & Cao Y, *J Sound Vib*, 494 (2021) 115790.
- 25 Wang W, Shi W, Thomas P, & Yang M, *Sensors*, 19 (2019) 137.
- 26 Padoin E, Fonseca J S O, Perondi E A, & Menuzzi O, *Lat Am J Solids Struct*, 12 (2015) 925.
- 27 Chen X, Yang T, Wang W, & Yao X, *Ceram Int*, 38 (2012) S271.
- 28 Bryant R G, Effinger I V R T, Aranda Jr I, Copeland Jr B M, & Covington III E W, *Proc SPIE*, 4699-40 (2002) 303.
- 29 Lai Y J, Li W C, Lin C M, Felmetsger V V, & Pisano A P, *Transducers Eurosensors XXVII*, (2013) 2268.
- 30 Shi Q, Wang T, Kobayashi T, & Lee C, *Cit Appl Phys Lett*, 108 (2016) 74109.
- 31 Mehdi-pour I, & Honarvar F, *Appl Math Model*, 91 (2021) 1141.
- 32 Li H, Liu D, Wang J, Shang X, & Hajj M R, *Energy Convers Manag*, 206 (2020) 112503.
- 33 Kumar R, *Measurement/monitoring of vibrations using digital speckle pattern interferometry*, Ph. D. Thesis, Indian Institute of Technology, New Delhi, 2003.
- 34 Bremerman J, Bronocco S, Caffey B, Kent T, Reed E, Lee E, Mukhopadhyay R, Patel A, Reed E, Rother C, Stambouli A, Verni E, & Wang T, Piezoelectric sensing and energy harvesting in touch screens, Gemstone Honors Program thesis, Maryland University, 2017.
- 35 Liu H, Lee C, Kobayashi T, Tay C J, & Quan C, *Sens Actuators A*, 186 (2012) 242.
- 36 Reis S, Correia V, Martins M, Barbosa G, Sousa R M, Minas G, Lanceros-Mendez S, & Rocha J G, *IEEE Intl Symp Ind Electron*, (2010) 516.
- 37 Elahi H, Eugeni M, & Gaudenzi P, *Adv Struct Mater*, 81 (2018) 35.
- 38 Mirza S, Singh P, Kumar R, Vyas A L, & Shakher C, *Opt Lasers Eng*, 44 (2006) 41.
- 39 Kumar R, & Shakher C, *Opt Lasers Eng*, 42 (2004) 585.